

Phenol Removal from Waste Water by Using a Commercial, Microporous Activated Carbon Granules (ACG)

Subrata Mondal, Yang Yang, and Kean Wang*

Department of Chemical Engineering, The Petroleum Institute, PO Box 2533, Abu Dhabi, United Arab Emirates

Abstract

A commercial microporous activated carbon granulate (ACG) was characterized and tested for phenol adsorption from water. The microstructure and surface chemistry of the ACG were characterized using N₂ adsorption, wide angle X-ray diffraction (WAXD), Raman, FTIR, TEM, SEM, and energy dispersive X-ray (SEM – EDX). The influences of ACG dosage, contact time, initial adsorbate concentration and salt concentration on phenol adsorption were studied in the batch mode. Experimental results revealed that: 1) The Freundlich equation and 2nd order kinetics are better models to describe the adsorption equilibrium and kinetics, respectively; 2) ACG presents a phenol capacity of ~ 90 mg/g at the dosage of 5g/L; 3) Phenol uptake on ACG involves both physical as well as chemical adsorption; 4) The adsorption capacity is sensitive to the presence of salts, particularly the divalent salt.

Key words: Adsorption, activated carbon, mechanism, phenol, water treatment.

Introduction

Industrial waste water containing phenolic compounds presents serious environmental/health hazards [1, 2],[3] and should be treated adequately before discharge to the environment. The adsorption process is a major technology while the activated carbon (AC) and activated carbon granules (ACG) are the most popular adsorbents in this type of wastewater treatment [4]. The ACG has a number of advantages such as: low-cost, availability, stability, durability, recyclability etc. [5]. The adsorption performance of AC/ACG largely depends on two of their properties: 1) porous structure (pore size and/or surface area), and 2) surface chemistry (functional groups). Such properties can be manipulated to some extent via the selection of carbon precursors, preparation processes, and the post treatments [6],[7-11]. For example, Srivastava et al. tested phenol adsorption on an AC derived from the sugarcane bagasse fly ash, and reported a adsorption capacity of 23.8 mg-phenol/g-AC at a phenol concentration of 55mg/L and a dosage of 10g/L [7]. An AC prepared from biomass (rattan sawdust) showed an capacity of 149 mg/g[8]. Removal of phenol from the petroleum industry's refinery wastewater by activated carbon revealed a high capacity of 262 mg/g[9]. This capacity as high as 303 mg/g[10] to 500 mg/g were also reported from some specifically prepared adsorbents[11]. In addition to the source of carbon, activation process also plays an important role. Activation of carbonaceous material derived from Kraft lignin with NaOH and KOH revealed

adsorption capacity of 238 and 213 mg/g, respectively [5]. Phenol uptake by activated carbon from the aqueous solution not only depends on its microstructure but also on the functional groups on the surface. For example, Fierro et al. reported a capacity of 238 mg/g on the NaOH-activated carbonaceous material, probably due to the existence of more functional groups [5]. This is expected as the phenol is a polar molecule, which can present strong electrostatic interaction with the functional groups on carbon surface, in addition to the physical adsorption in the porous networks.

Methods and Materials

Materials: The ACG sample was obtained from BPL, Calgon Corporation. Phenol was obtained from the Merck. All other chemicals are of analytical grade. Deionized water was used for all experimental purposes.

Characterizations: Fourier transform infrared (FTIR) spectra were obtained using an ATR-FTIR spectrometer (Vertex 70, Bruker) by averaging 128 scans in the 4000 – 400 cm⁻¹ spectral ranges at 4 cm⁻¹ resolution. Powder X-ray diffraction (XRD) spectrum of ACG was analyzed using an Analytical X'Pert PRO powder Diffractometer. Raman analysis was carried out using a Jobin Yvon Horiba LabRAM spectrometer with back-scattered confocal configuration. N₂ isotherm (at 77K) was measured on the sample using a pore and surface analyzer (Quantachrome

* Corresponding author

Email: yayang@pi.ac.ae;

©2016 International Association for Sharing Knowledge and Sustainability

DOI: 10.5383/swes.8.02.001

Autosorp-1, USA). Prior to the experiment, the sample was degassed at 120 °C and 10^{-5} Torr for 6 hours. The pore size distributions and cumulative pore volume were obtained from the Barrett-Joyner-Halenda(BJH) method [12]. Scanning electron microscope (SEM, JSM) was employed to observe the surface morphology of native and phenol-loaded ACGs. The samples were observed at various magnifications, with simultaneously elementary analysis by the Energy Dispersive X-ray Spectroscopy (EDAX). Transmission electron microscopy (TEM) studies were performed in a FEI Tecnai 20 ST electron microscope (1.1 Å point resolution), equipped with an EDAX microanalysis system for X-ray energy dispersive spectroscopy (EDS) and a GIF for electron energy loss spectroscopy (EELS) experiments.

Results and Discussion

Characterization of ACG: FTIR spectra (Figure 1) show that the broad and weak peak at around 3400 - 3900 cm^{-1} is due to the O - H vibration of hydroxyl groups. The weak and broad peak in the region of 1700 cm^{-1} could be assigned to the C=O stretching of carboxylic functionalities [13]. Phenolic type C - H peak appeared at $\sim 2920 \text{ cm}^{-1}$ [14]. Peak at $\sim 2340 \text{ cm}^{-1}$ is due to the asymmetric stretch of CO_2 existed in the activated carbon sample. Figure 2 shows the X-ray diffraction pattern of ACG. Broad asymmetric peaks were spotted at $23.5\text{-}26.7^\circ$ (2θ) and at 43.7° (2θ), which are typical for amorphous carbons with graphite units and could be assigned to the disordered graphitic $\{002\}$ and $\{100\}$ planes, respectively [15-17]. In addition, a weak $\{004\}$ peak was spotted at $\sim 35^\circ$.

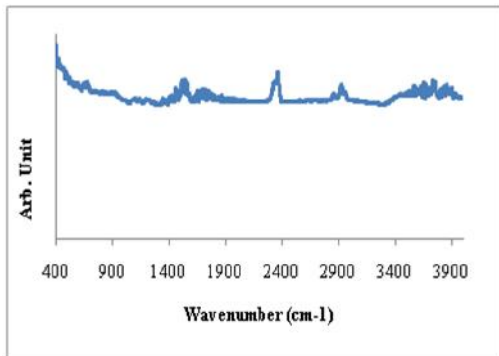


Figure 1: FTIR of the original ACG

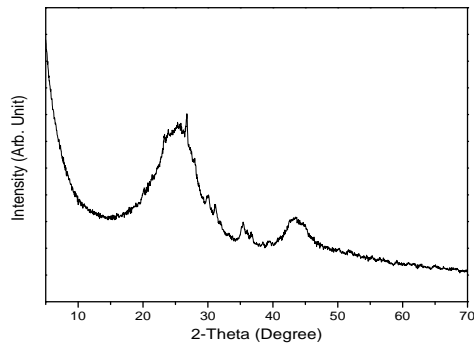


Figure 2: XRD Pattern of Original Activated Carbon Granules

Two sharp Raman peaks (Figure 3), the G (graphite)-band and the D (disorder)-band, appeared at approximately 1580 and 1320 cm^{-1} , respectively. The G- band is associated with the vibration of sp^2 carbon atoms and corresponds to the high degree of symmetry and order of carbon materials. The D-band corresponds to the vibration of sp^3 carbon atoms of defects and disorder in the curved graphite sheet[18]. The intensity ratio of D to G peak (ID/IG) is ~ 1.103 , which shows that the ACG is largely amorphous.

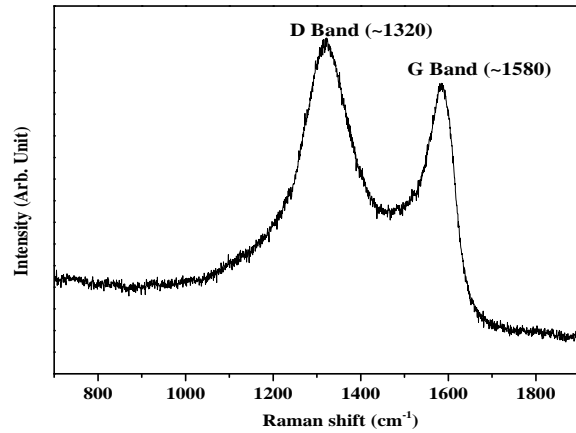


Figure 3: Raman Spectroscopy of the ACG

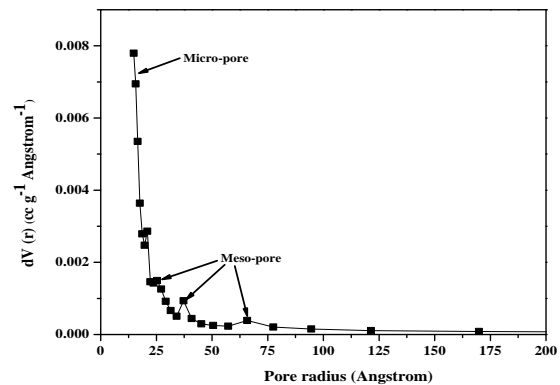
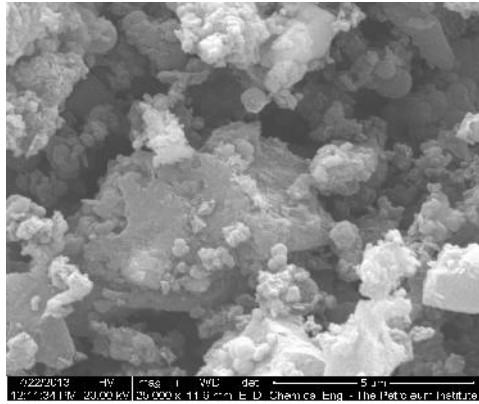
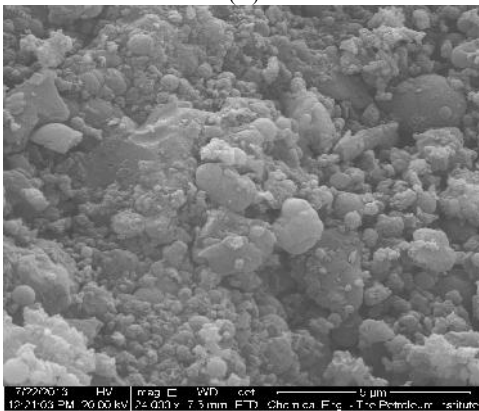


Figure 4: Pore Size Distribution of the ACG

Figure 4 and Table 1 present the structural characteristics of the ACG. It is seen that the ACG is essentially microporous (with the major peak of pore size $< 2 \text{ nm}$). Small mesopore peaks were also spotted around 3 and 6 nm. Such mesopores generally exist between graphite units and play important role for interparticle diffusion [19].



(A)



(B)

Figure 5: SEM Micrographs of ACG (A) before Phenol Adsorption and (B) after Phenol Adsorption

Figures 5 show the SEM surface morphology of the ACG before and after phenol adsorption respectively. It is seen that ACG had a significant open structure before adsorption (5a), which became densely packed after adsorption (5b). This observation suggests that adsorbed phenol molecules collapsed/blocked some of the porous structure [17]. EDX results (Table 1) revealed that native sample

Table 1 The Characteristics of ACG Sample

BET Analysis (Native ACG samples)		EDX Analysis	
Characteristics	Values	Elements	Concentration (% w/w)
BET surface area (m ² /g)	1,024	Original ACG	93.4
Total pore volume (cm ³ /g) at P/Po = 0.99	0.59	O	6.7
		Phenol loaded ACG	
		C	94.3
Average pore diameter (Å)	~12	O	5.7

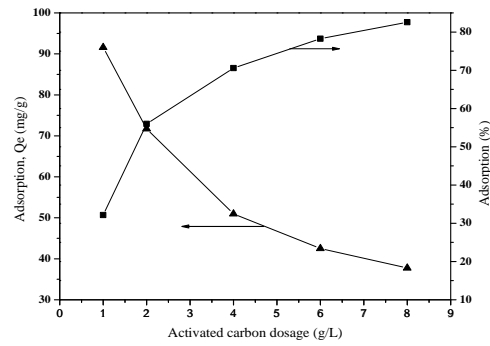


Figure 6: Effect of ACG dosage on adsorption of phenol [C₀ = 150 mg.L⁻¹, ACG dosage 1-8 g.L⁻¹, adsorption time: 24 h, Adsorption, Q_e; Adsorption (%)]

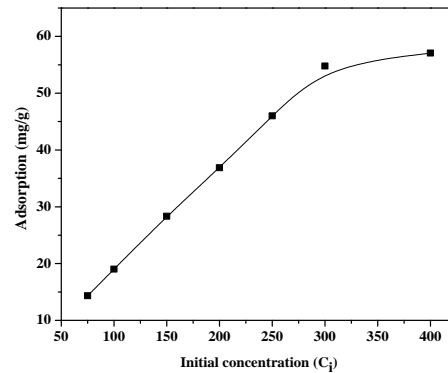


Figure 7 Influence of Initial Phenol Concentration C₀ on ACG [C₀ = (75 – 300) mg.L⁻¹, ACG Loading: 5 g.L⁻¹, Adsorption Time: 16 h];

has some oxygen groups on its surface. Oxygen functional groups (e.g. C=O, –COOH etc.) are very important characteristics of the activated carbons because they play an important role in the surface chemistry and thereby affect phenol adsorption.

Influence of adsorbent dosage: Figure 6 show that the adsorption efficiency (%) increases with the increase of adsorbent dosage (g-ACG/L) till a plateau is reached, while the adsorption capacity decreases gradually. This is in line with the expectation that higher dosage corresponds to more adsorption sites [14]. The residual concentration of phenol is high at low dosage due to the saturation of adsorbent [20]. The initial experimental result revealed that a dosage of 5 g/L is enough for the quantitative removal of phenol with the ACG sample, and therefore, was fixed for the rest of the experiments.

Adsorption Isotherms: Figure 7A plots the phenol adsorption vs the initial phenol concentration. It is seen that, when the initial concentration increases, the adsorption (Q_e) increases linearly while adsorption efficiency (%) decreases slightly (95.39% adsorption at C_i 75 ppm and 91.28% adsorption at C_i of 300 ppm). With the higher initial phenol concentration, the mass transfer driving force hence the rate at which phenol molecules diffuse from the bulk solution to the activated carbon surface increases [21]. Meanwhile, at higher adsorbate concentration, the capacity of the adsorbent approaches saturation, resulting in decrease in

overall removal [2]. Adsorption isotherm is important to describe how adsorbate molecules interact with the adsorbent, and is critical in optimizing the system design. Two popular isotherm models, i.e. Langmuir and Freundlich are fitted to the experimental data. The Langmuir model is applicable to a homogeneous surface with monolayer adsorption [1, 8], while the Freundlich isotherm model is more applicable for adsorption on a heterogeneous surface. The fitting results are listed in Table 2.

Table 2 Isotherms and Kinetics Parameters for Phenol Adsorption on ACG

Isotherm	Isotherm parameters	Kinetic constants
Langmuir $C_{\mu} = \frac{Q_0 b C}{1 + b C}$	$Q_0 = 90.1 \text{ mg/g}$ $b = 0.047 \text{ L/mg}$ $R^2 = 0.95$	Pseudo-first-order constants $k_1 = 0.2341 \text{ (h}^{-1}\text{)}$ $R^2 = 0.95$
Freundlich $C_{\mu} = K_F C^{1/n}$	$n = 1.57$ $K_F = 6.8$ $(\text{mg/g})(\text{L/mg})^{1/n}$ $R^2 = 0.99$	Pseudo-second-order constants $k_2 = 0.091 \text{ g.mg}^{-1}.\text{h}^{-1}$, $R^2 = 1$

We see in Table 2 that the Freundlich equation gives a better fit ($R^2 = 0.99$) vs Langmuir ($R^2 = 0.95$) equation. This may suggest that surface of ACG presents a certain degree of heterogeneity, largely due to the existence of functional groups, as revealed by the previous characterization results[22].

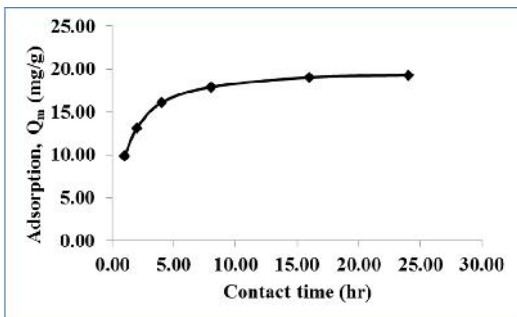


Figure 8A: Effect of Contact Time on Phenol Adsorption by ACG

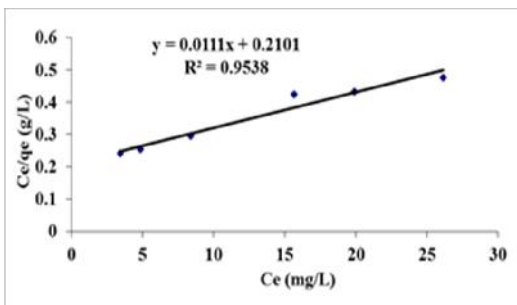


Figure 8B: 1st order Kinetic Model of Phenol Adsorption on ACG

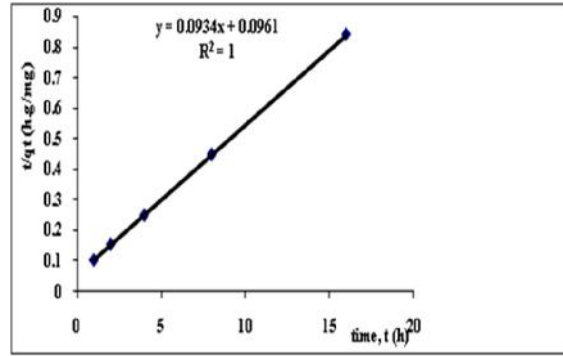


Figure 8C: 2nd Order Kinetic Model of Phenol Adsorption on ACG

Adsorption kinetics: Figures 8 shows the rate of phenol adsorption at the initial concentration of 100 ppm. The experimental result suggests that the curves rise sharply in the initial stages, until a plateau is reached (8A)[1,8]. Adsorption kinetics are dictated by the underlying adsorption mechanisms [23] and are generally represented by either pseudo 1st order (8B) or the 2nd order (8C) kinetic equations. In general, the 2nd order equation is based on the adsorption rate control over the whole long time range. Table 2 revealed that the 2nd order equation fits the experimental data slightly better ($R^2 \sim 1$) than that the 1st order model[8].

Influence of ion concentration: The industrial effluent contains many salts together with organic pollutants. Dissolved salts in the aqueous media often influences adsorption capacity [4]. Therefore, NaCl and Na₂SO₄ were used as the model salts to investigate their influence (ionic strength) on the phenol adsorption. It is seen in Figure 9 that NaCl plays a relatively stable role (~ 10% decrease in phenol capacity when its dosage increases from 1 to 8 g/L), while sulphate (SO₄²⁻) plays a significant role (a decrease of ~ 20% at the dosage of 8 g/L). This capacity decrease is caused by the ions which block the microporous structure (physical adsorption) and interact with the functional groups on ACG's surface (chemical adsorption) [12]. Because sulphate possesses a large molecular size and more charges, it exerted a stronger influence on phenol uptake than its counterpart.

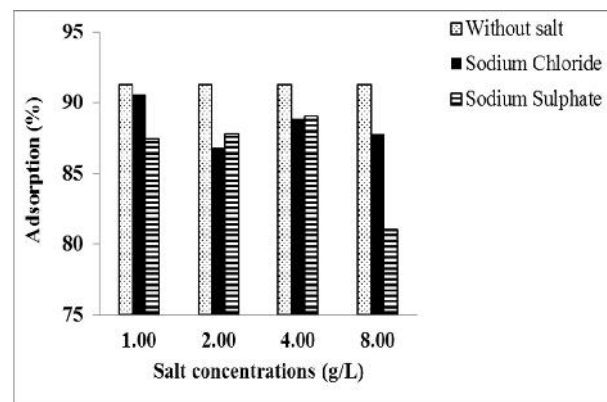
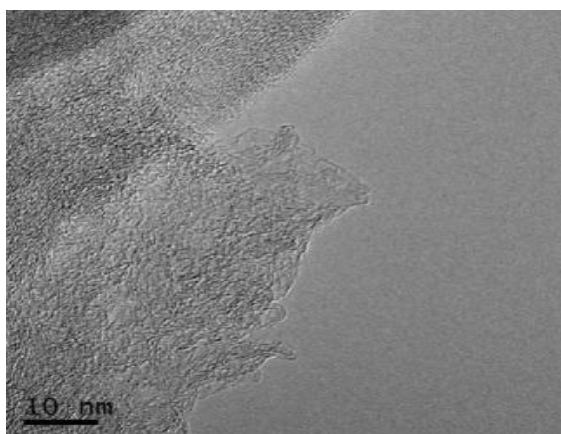


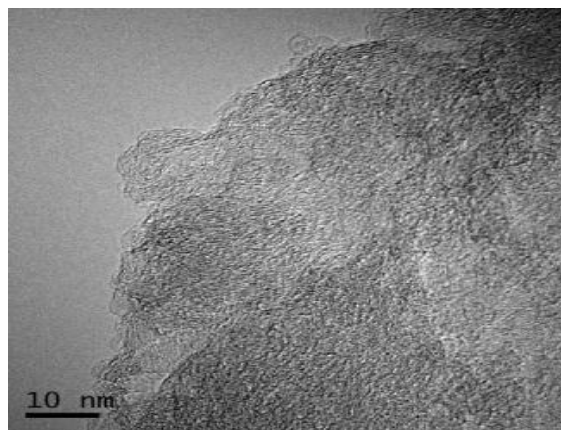
Figure 9: Influence of Two Salts on the Adsorption of Phenol by ACG (Phenol Conc: 300 mg/L, ACG dosage: 5 g/L, Adsorption Time: 16 h)

Mechanism of phenol adsorption on ACG: Phenol adsorption on carbon is a complicated process, which depends on the surface area, pore size, pore volume and surface functional groups of the adsorbent. The phenol molecule consists of the aromatic ring and

hydroxyl group (-OH) which is an electron donor. Therefore, the presence of carboxylic group (-COOH) and other oxygen containing groups (as indicated by FTIR spectra) on the activated carbon surface would enhance the interaction/adsorption by the ester bond formation between the two type of functional groups. The physical adsorption occurs mainly due to the dispersive interactions between the benzene ring and the basal graphite plane [6], which is a strong function of the pore size. Other electrostatic attraction may include: H-bonding, dipole-dipole and dipole-induced dipole interactions, etc. [24]. In addition to these, phenol adsorption could also occur due to the diffusion of phenol molecules from the aqueous solution to the porous structure of the activated carbon. Porosity of the activated carbon granules takes a major driving role for the adsorption of phenol from the aqueous solution. The pore adsorption mainly takes place in ultramicropores ($d < 0.7$ nm) and micropores ($d < 2$ nm), which are similar in size as compared with the molecular diameter of phenol (kinetic molecular diameter of phenol is around 0.62 nm) [13]. However, as only few of them are presents on the outer surface. Therefore, both micropores and mesopores are also important for the passage of the phenol molecules to the micropores/ultra-micropores [25].



(A)



(B)

Figure 10: TEM Images of the (A) Native and (B) Phenol Loaded ACG Samples

The TEM images of the native and phenol loaded ACGs are shown in Figures 10. The predominant microporosity of the ACG gives a largely homogeneous morphology view. The bright shapes are considered to be the pores. It is seen in Figure 10A that the native sample has a typical turbostratic, disordered porous

microstructure with tightly curled carbon layers. Some wider spaces are found among the hexagonal stacks near the surface, which may reflect the mesopores. After adsorption, it is seen in Figure 10B that surface morphology has significantly changed due to the load of phenol molecules [26]. The local chemical composition for particle obtained using X-ray EDS showed that the native sample has an atomic % C and O % of 97.7 and 2.03, respectively. After adsorption with phenol, the atomic % C content increased to (98.67%) while that of O dropped to 1.32 due to the influence of aromatic phenol molecule (C_6H_5OH) on adsorbents.

Conclusions

The activated carbon granule possesses a microporous structure and complicated surface chemistry. The adsorption equilibrium is better described by the Freundlich isotherm, suggesting a heterogeneous surface towards phenol molecules. The adsorption kinetics was represented by the pseudo-second-order kinetic models. The addition of divalent salt drastically reduces the phenol adsorption both physically and chemically. SEM and TEM results revealed that both physical and chemical adsorption may play important roles on phenol adsorption on the sample.

References

- [1] L. J. Kennedy, J. J. Vijaya, K. Kayalvizhi, and G. Sekaran, "Adsorption of phenol from aqueous solutions using mesoporous carbon prepared by two-stage process," *Chemical Engineering Journal*, vol. 132, pp. 279-287, Aug 1 2007.
- [2] S. P. Kamble, P. A. Mangrulkar, A. K. B. Ansiwal, and S. S. Rayalu, "Adsorption of phenol and o-chlorophenol on surface altered fly ash based molecular sieves," *Chemical Engineering Journal*, vol. 138, pp. 73-83, May 1 2008.
- [3] Y. A. Alhamed, "Adsorption kinetics and performance of packed bed adsorber for phenol removal using activated carbon from dates' stones," *Journal of Hazardous Materials*, vol. 170, pp. 763-770, Oct 30 2009.
- [4] H. A. Arafat, M. Franz, and N. G. Pinto, "Effect of salt on the mechanism of adsorption of aromatics on activated carbon," *Langmuir*, vol. 15, pp. 5997-6003, Aug 31 1999.
- [5] V. Fierro, V. Torne-Fernandez, D. Montane, and A. Celzard, "Adsorption of phenol onto activated carbons having different textural and surface properties," *Microporous and Mesoporous Materials*, vol. 111, pp. 276-284, Apr 15 2008.
- [6] Salame, II and T. J. Bandosz, "Role of surface chemistry in adsorption of phenol on activated carbons," *Journal of Colloid and Interface Science*, vol. 264, pp. 307-312, Aug 15 2003.
- [7] V. C. Srivastava, M. M. Swamy, I. D. Mall, B. Prasad, and I. M. Mishra, "Adsorptive removal of phenol by bagasse fly ash and activated carbon: Equilibrium, kinetics and thermodynamics," *Colloids and Surfaces a-Physicochemical and Engineering Aspects*, vol. 272, pp. 89-104, Jan 5 2006.
- [8] B. H. Hameed and A. A. Rahman, "Removal of phenol from aqueous solutions by adsorption onto activated carbon prepared from biomass material," *Journal of Hazardous Materials*, vol. 160, pp. 576-581, Dec 30 2008.

- [9] M. H. El-Naas, S. Al-Zuhair, and M. Abu Alhaja, "Removal of phenol from petroleum refinery wastewater through adsorption on date-pit activated carbon," *Chemical Engineering Journal*, vol. 162, pp. 997-1005, Sep 1 2010.
- [10] C. O. Ania, J. B. Parra, and J. J. Pis, "Effect of texture and surface chemistry on adsorptive capacities of activated carbons for phenolic compounds removal," *Fuel Processing Technology*, vol. 77, pp. 337-343, Jun 20 2002.
- [11] P. Girods, A. Dufour, V. Fierro, Y. Rogaume, C. Rogaume, A. Zoulalian, et al., "Activated carbons prepared from wood particleboard wastes: Characterisation and phenol adsorption capacities," *Journal of Hazardous Materials*, vol. 166, pp. 491-501, Jul 15 2009.
- [12] F. B. Su, L. Lv, T. M. Hui, and X. S. Zhao, "Phenol adsorption on zeolite-templated carbons with different structural and surface properties," *Carbon*, vol. 43, pp. 1156-1164, May 2005.
- [13] U. Beker, B. Ganbold, H. Dertli, and D. D. Gulbayir, "Adsorption of phenol by activated carbon: Influence of activation methods and solution pH," *Energy Conversion and Management*, vol. 51, pp. 235-240, Feb 2010.
- [14] A. Gundogdu, C. Duran, H. B. Senturk, M. Soylak, D. Ozdes, H. Serencam, et al., "Adsorption of Phenol from Aqueous Solution on a Low-Cost Activated Carbon Produced from Tea Industry Waste: Equilibrium, Kinetic, and Thermodynamic Study," *Journal of Chemical and Engineering Data*, vol. 57, pp. 2733-2743, Oct 2012.
- [15] B. Zhang, T. Wang, S. Liu, S. Zhang, J. Qiu, Z. Chen, et al., "Structure and morphology of microporous carbon membrane materials derived from poly(phthalazinone ether sulfone ketone)," *Microporous and Mesoporous Materials*, vol. 96, pp. 79-83, Nov 26 2006.
- [16] M. W. Jung, K. H. Ahn, Y. Lee, K. P. Kim, J. S. Rhee, J. T. Park, et al., "Adsorption characteristics of phenol and chlorophenols on granular activated carbons (GAC)," *Microchemical Journal*, vol. 70, pp. 123-131, Nov 2001.
- [17] C. Namasivayam and D. Kavitha, "IR, XRD and SEM studies on the mechanism of adsorption of dyes and phenols by coir pith carbon from aqueous phase," *Microchemical Journal*, vol. 82, pp. 43-48, Jan 2006.
- [18] S. Chen, J. Hong, H. Yang, and J. Yang, "Adsorption of uranium (VI) from aqueous solution using a novel graphene oxide-activated carbon felt composite," *Journal of Environmental Radioactivity*, vol. 126, pp. 253-258, Dec 2013.
- [19] A. P. Terzyk, "Further insights into the role of carbon surface functionalities in the mechanism of phenol adsorption," *Journal of Colloid and Interface Science*, vol. 268, pp. 301-329, Dec 15 2003.
- [20] C. Hua, R. Zhang, L. Li, and X. Zheng, "Adsorption of phenol from aqueous solutions using activated carbon prepared from crofton weed," *Desalination and Water Treatment*, vol. 37, pp. 230-237, Jan 2012.
- [21] H. B. a. A. A. Maarof HI, "Adsorption isotherms for phenol onto activated carbon," *AJChE*, vol. 4, pp. 70-76, 2004.
- [22] W. F. C. Juang R –S, Tseng R –L, "Adsorption isotherms of phenolic compounds from aqueous solutions onto activated carbon fibers," *Journal of Chemical Engineering Data*, vol. 41, pp. 487-492, 1996.
- [23] W. J. T. a. C. RK, "Pore and solid diffusion model for fixed bed adsorber," *Journal of American Institute of Chemical Engineering*, vol. 2, pp. 228-238, 1974.
- [24] A. H. Sulaymon, D. W. Abbood, and A. H. Ali, "Removal of phenol and lead from synthetic wastewater by adsorption onto granular activated carbon in fixed bed adsorbers: prediction of breakthrough curves," *Desalination and Water Treatment*, vol. 40, pp. 244-253, Feb 2012.
- [25] Z. Ioannou and J. Simitzis, "Adsorption kinetics of phenol and 3-nitrophenol from aqueous solutions on conventional and novel carbons," *Journal of Hazardous Materials*, vol. 171, pp. 954-964, Nov 15 2009.
- [26] P. J. F. Harris, Z. Liu, and K. Suenaga, "Imaging the atomic structure of activated carbon," *Journal of Physics-Condensed Matter*, vol. 20, Sep 10 2008.